Spiral arm lanes as seen from young and old stellar tracers

Author: Joseph David Altamirano Bonilla
*Facultat de Física, Universitat de Barcelona, Diagonal 645, 08028 Barcelona, Spain.**

Advisor: Francesca Figueras Siñol
(Dated: June 23, 2021)

Abstract: In this work we compare the spiral structure depicted by two stellar tracers with very different ages: an extremely young population of OB type stars and a population of Red Clump stars assumed to be relaxed in the Galactic potential. A Kernel density estimator applied to Gaia and StarHorse EDR3 data allow us to trace the over/under-density maps on the Galactic plane at ± 3 kpc from the Sun location. Preliminary results confirm that Perseus and Sagittarius-Carina arms are well delineated in both samples and possible offsets between their locus are evaluated. More important, the surface density amplitude of the young population is estimated to be a factor 2-3 larger than that of the old population. These results provide new insights to discern on the mechanisms by which the Milky Way spiral arms evolve.

I. INTRODUCTION

As a starting point for this work we might start talking about our Galaxy, specifically about its shape and structure. It is well know that the Milky Way is a spiral barred galaxy. The arms are inside a flat thin disc surrounded by a thick disk and an almost spherical halo, which different types of stars inhabiting each of these structures. We are interested in the thin disc, where the spiral structure was formed and is been evolving. The nature and mechanism for this spiral structure is still a matter of debate in the present days and, as an example. several geometric model for its structure has been proposed (e.g. [**?** **?**]. In the Gaia era new data allow us to analyze a larger area around the Sun (e.g. [1], [8]). Our work tries to contribute to this effort by studying and comparing the geometry of the spirals as traced by two stellar populations with very ages in this surrounded area.

For our work we select two populations, a Upper Main Sequence population (hereafter UMS), composed by massive and intrinsically bright young (ages $<$ 200 Myr) OB type stars, and an evolved population of Red Clump stars, with ages in the rang 1-6 Gyr. Since we use stars formed at considerably different times we think they analysis and comparison can glimpse the mechanisms of evolution of the structure of the arms. As an example, we wonder if there exist an offset in the location of the over/under-densities through or across the arm, as widely discussed in the literature between the dust layer and the young population (e.g. [10]). We want also to quantify the amplitude of this over/under-densities and compare results derived from the two different tracers. These are contributions that can help to understand or discern about the different mechanisms proposed for the evolution of these structures (e.g. density wave theory, cor-rotating arms, etc).

In order to be able to do it, we will use recent and accurate data released in December 2020 by the GAIA space observatory. Using this data we will compare the over/under-density of stars from the UMS ($T_{eff} \gtrsim 10.000$ K) and the RC (4.500 K $\leq T_{eff} \leq$ 5.000 K), two very different populations, with the RC evolved over time. We suspect that they are concentrated in regions significantly different from the young ones. For the purpose to the comparison be as valid as possible, we will use the same methodology, by utilizing a kernel density estimation[2] to make over/under-density maps from both data sets with the same strategy and the same parameters.

In Section II we will detail the kernel function to be used and the UPM and RC samples. In Section III we present and discuss the resulting maps, the first look differences between UMS and RC and the obtained spiral arms amplitudes. Section IV present the conclusions and future work.

II. METHODS AND STELLAR TRACERS

A. Over/under-density maps

We use the Epanechnikov kernel density estimation (1) to trace the over/under-density maps in the Galactic plane. It is a non-parametric function which gives us the local density [2]. By means of the Epanechnikov function we calculate the density in a 2D plane via equation (2). This kernel function in 2D has been recently used by E. Poggio et al. in [1]:

$$K(\frac{\mathbf{X}-\mathbf{x_i}}{h}) = \begin{cases} \frac{3}{4}(1-(\frac{\mathbf{X}-\mathbf{x_i}}{h})^2) & \frac{\mathbf{X}-\mathbf{x_i}}{h} \leq 1 \\ 0 & \frac{\mathbf{X}-\mathbf{x_i}}{h} > 1 \end{cases}, \quad (1)$$

*Electronic address: jaltambo7@alumnes.ub.edu

$$\Sigma(\mathbf{X},\mathbf{Y}) = \frac{1}{Nh^2}\sum_{i=1}^{N}[K(\frac{\mathbf{X}-\mathbf{x_i}}{h})K(\frac{\mathbf{Y}-\mathbf{y_i}}{h})]. \quad (2)$$

Where $(\mathbf{x_i}, \mathbf{y_i})$ are the coordinates of each star in the xy plane, N is the number of stars, $(\mathbf{X}, \mathbf{Y})$ are the coordinates of the plane where the kernel function is computed and h is the bandwidth of its function. From that, we define the over/under-density as:

$$\Delta_\Sigma(\mathbf{X},\mathbf{Y}) = \frac{\Sigma(\mathbf{X},\mathbf{Y})_1 - \Sigma(\mathbf{X},\mathbf{Y})_2}{\Sigma(\mathbf{X},\mathbf{Y})_2}, \quad (3)$$

where Σ_1 and Σ_2, defined in the equation (2), differ by its h value, being $h_1 < h_2$. Therefore, the over/under-density is defined as the difference between the local density and the mean density, with respect to these mean density. Finally, with this over/under-density equation (3) we can elaborate different maps, selecting in each case, the appropriate bandwidths parameters.

The value of the bandwidths parameters will be fixed depending on the size of the structures and the kind of stellar tracers we are interested to enhance to proceed with the comparison of the the resulting maps; the value of h_1 determine the average size of the smallest structures we are able to discern, whereas the one of h_2 determine the area over which is the density averaged. We proceed empirically until we reach a final conclusion on the optimal h_1 and h_2. As mentioned, our main goal is to study the large scale structures associated to the spiral arms in the solar neighbourhood. With that in mind, we have created many maps with different combinations of those parameters until we reached to conclude that:

- h_1 has to be between $(0,1 \sim 0,2)$ kpc, the mean size of the star formation regions and/or the spiral arms width [3]
- h_2 has to be related to the separation between spiral arms in our study region, on the order of 1-2 kpc, as seen in the maps created later.

After several tests we have decided to use $h_2 = 1$ kpc since if it is larger, the edges of the larger structures become more blurred. The selection of $h_2 = 1$ kpc implies to use all the stars in the catalogue located inside the ± 4 kpc map.

We want to generate the overdensity maps between ± 3 kpc from the Sun location in both $(\mathbf{X}, \mathbf{Y})$ axes. In this manner we are able to include regions like the Perseus Arm, the Local Arm, the Carina-Sagittarius Arm and specially some tracers of star formation like the Cepheus Spur and the Cygnus and Vela associations, among others. But we have to be aware that this range in $(\mathbf{X}, \mathbf{Y})$ is so wide that radial extinction effects at low Galactic latitudes would be predominant in some Galactic longitude directions. This effect occurs when the dust and the interstellar gas extinct the radiation from far bright stars. In our case for both, UMS and RC tracers, these effects can have important consequences in the spatial distribution we plan to study. Lastly, is noteworthy that our ± 3 kpc maps will be in the Cartesian galactic coordinates and with the Sun centered on (0, 0, 0) kpc. In this coordinate system, the Galactic center is at (8.2, 0, 0) kpc.

B. The Upper Main Sequence Stars

The young OB stars catalogue used in this work is the one recently published in [1]. It contains 606.996 stars for which Bayesian distances have been recomputed using the new Gaia EDR3 astrometry. Our first task has been to check that we reproduce the XY maps published in this paper. The stars inside this data set are very young stars, located above all in the thin disc, most of them belonging to the nearby star-forming regions such as Cygnus, Perseus, Cepheus and others. These are the structures modeling the young spiral arms in the solar neighbourhood. We refer to [1] and/or [11] for an extensive description of these regions. We present the XY over/under-density maps of this UMS population in the top panels of Fig. 1. It should be noted that there is an artificial lack of stars in the vicinity of the Sun ($r < 0.2$ kpc) due to the data cone-shaped collection itself (see [1] for a detailed explanation).

C. The Red Clump population

Thanks to F. Anders we have had early access to the StarHorse EDR3 catalogue ([6]). We have selected the RC sources with the following criteria: 1) RC stars between $T_{eff} = [4500, 5000]$K and $logg = [2,35, 2,55]$ dex; with $[Fe/H]$ in the range [-0.6, +0.4] dex to avoid stars coming from the halo or the thick disc, and $|Z| < 0.5$ kpc With these cuts we concentrate our sample to stars coming from the thin disc, inasmuch as the population from the thick disc mainly have lower metallicity and a higher distribution in Z. In the Appendix we present a detailed description of the improvements on the Bayesian distances in this new StarsHorse EDR3 catalogue.

III. RESULTS

A. Maps ± 3 kpc

By using equation (3) with $h_2 = 1,0$, we have generated two over/under-density maps for each data set using, respectively, $h_1 = 0,1$ kpc and $h_1 = 0,2$ kpc. Results are presented in Fig. 1. The grid of points for which the kernel is computed are separated by a distance of 0.020 kpc, therefore, although it may seem like a

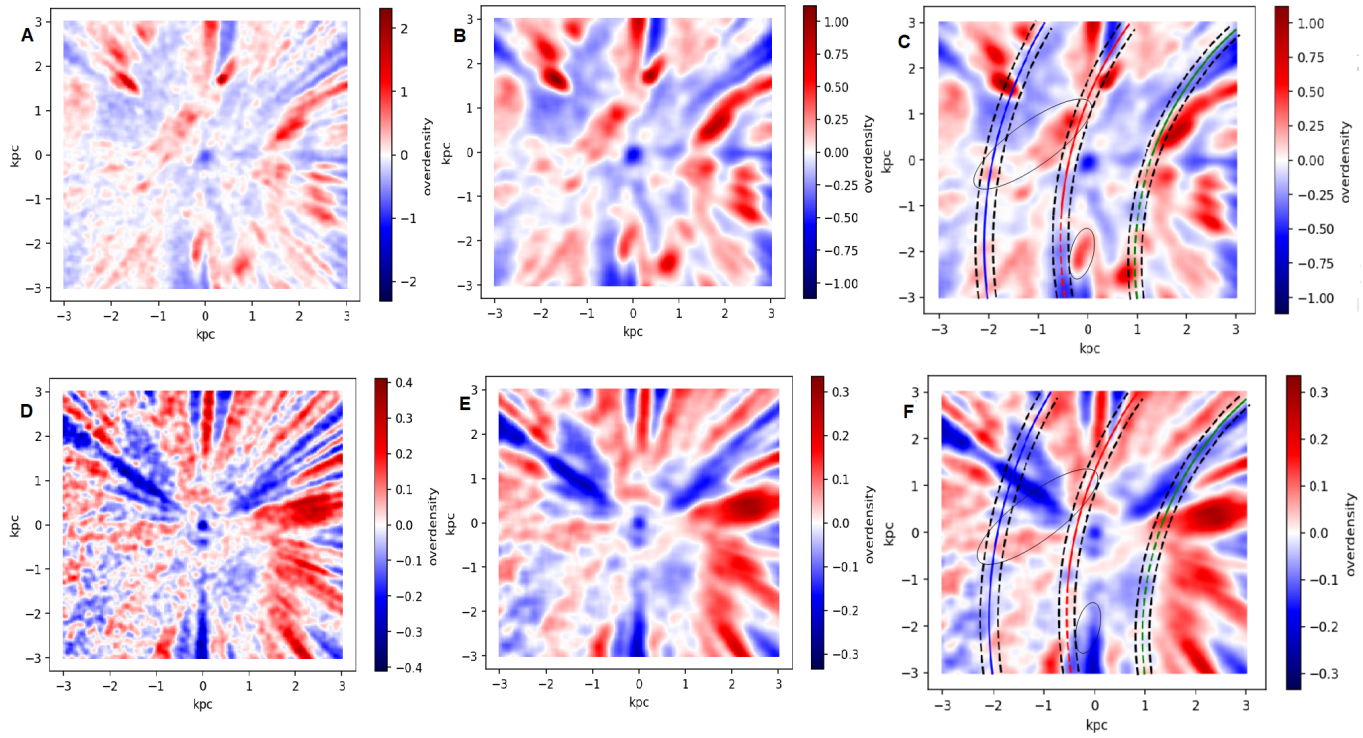

FIG. 1: Over/under-density maps projected on the $(\mathbf{X}, \mathbf{Y})$ plane for the UMS (top) and RC (bottom) populations. Maps have been calculated using Eq. 3 with $h_2 = 1,0$ kpc. Panel A and D uses $h_1 = 0,1$ kpc whereas B i E $h_1 = 0,2$. Panel C and F reproduce panel B and E, respectively, but with the geometrical model for the spiral arms by [3]. We have also superimposed on top the ellipses with the location of the Cepheus spur and Vela OB1 association (see [4]. The X axis is positive toward the galactic center and the Y axis towards the Galactic rotation

.

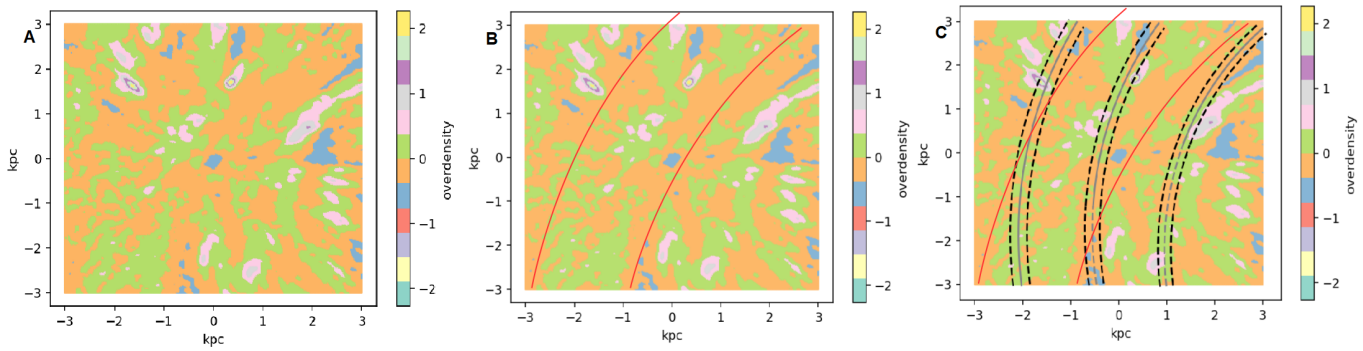

FIG. 2: Panel A: Differences between the over/under-density color maps of the two populations (UMS minus RC). Maps have been generated using Eq. 4 and $h_1 = 0,1$ kpc. Panel B: As panel A, but with two curved lines hand-traced to highlight the regions presenting a continuous negative value. Panel C: The same as B, but with the [3] spiral arm geometrical model

smoothed image, each observable point corresponds to a calculated value.

As a first important result we realize that both tracers, UMS and RC, present the clear large scale structures of the Perseus and Carina-Saggitarius arms. Other known structures such as the Local Arm, and the star forming regions of Cygnus and Vela are easily identifiable in the UMS maps (Panels A, B and C).

We observe that the previously commented hole in the center, which has a diameter about 0,3 kpc, is well observed in the two samples. As mentioned this is an artificial phenomena that apart from creating this non-real underdensity, enhances the overdensity in its neighborhood. Nevertheless, we think this handicap

does not disturb too much the large scale structures discussed in this section. This lack of stars in the center is known and well located. For the same reason, we notice a great accentuation in the overdensity inside the star-forming regions, which makes the other dots look less intense, but this effect is reduced when h_1 increases, by the intrinsic nature of the equation (3)

Focusing on the RC maps, it is important to emphasize that the scale is about one order of magnitude below that of the UMS stars. Contrary to what happens for the UMS stars, we observe that the RC stars shows no great accentuation in the values, rather, the over/under-densities are not as much localized as the UMS ones. To understand more these effects in .3 we present the 1D histograms of the over/under densities plotted in Fig. 1. These plots have been done to quantify and compare the amplitude of the spirals in the solar neighbourhood for the two tracers, UMS and RC. Our results allow us to quantify, for the first time, that the amplitude of the stellar density provoked by the spiral arms for the young population (UMS) is a factor 2-3 that of the RC, a population already relaxed in the Galactic potential. Another important feature observed in the UMS histogram is the skewness, a asymmetry in the overdensity distribution associated to the star forming regions (Perseus, Cygnus and Vela). It is this low amplitude of the RC sources what accentuates the effects due to the interstellar extinction. For this population, as can be seen in the D, E and F panels, the under/over-densities are more affected by this phenomena.

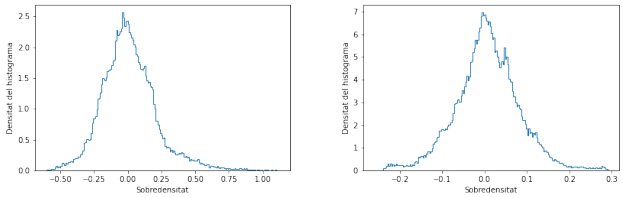

FIG. 3: 1D Histogram of the over/under densities for the UMS (left) and RC (right) plotted in Fig. 1

Whereas it is clear that, as mentioned above, the major arms can be distinguished in the under/over-densities structures, in panels D) and F) we can see how these arms for UMS and RC differ from the model arms location proposed by [3]. The main reason, already discussed in [11], among others, is that this model is based on H-II regions and massers, thus reproducing the location of the extreme young population and gas. Besides, the colored dashed line refers to the fact that the [3] model is not available for this region, thus the extension we have done shall be considered as a rough approximation. And the black dashed lines mean the model arm width proposed by [3].

B. A first comparison of the UMS and the RC spiral arms

First we focus on panels C and F from Fig. 1. Here we can see how despite the fact that the two populations have some coherence with the superimposed models on the major arms, as expectec, the RC overdensities seems to differ more from this model than the UMS. It seems that the overdensities RC associated, both those associated to Perseus (external arm) and those to Carina-Sagittarius (inner arm), are a bit displaced to the Galactic center. Nontheless this is only a qualitative evaluation. With the aim to quantify this effect we define de difference on over/under-density between the two populations as:

$$\Lambda_{h1}(\mathbf{X},\mathbf{Y}) = \Delta_{\Sigma,UMS}(\mathbf{X},\mathbf{Y}) - \Delta_{\Sigma,RC}(\mathbf{X},\mathbf{Y}). \quad (4)$$

where $\Delta_{\Sigma,i}$ is defined in equation (3). Results are presented in Fig. 2Fig.2. In panel A we identify mainly two regions: a negative regions (orange, negative values) where the overdensity from the RC stars dominates the underdensity from UMS stars, and another (green, positive) where occurs the opposite. For simplicity, if we focus our attention to the negative values, we observe a continuous trend inclined respect to the geometrical model of [3]. In panel B we highlighted the lanes (hand traced) where this negative value are continuous and remains, which matches with the region where the UMS map has underdensities and the RC map has a noticeable overdensity, that is regions where the population is mainly RC. Lastly, in panel C we superimposed these new curves with the spiral arms model for maser sources proposed by [3]. What we found is that mainly in the first, second and fourth galactic quadrants (defined from the Galactic center and on counter-clock wise) the curves present a large pitch angle than the geometrical model. Finally, maybe this would lead us to think that these curves trace the dominance of the RC over the UMS stars and the stars over time are relaxing and end up positioning themselves in those potential well regions.

Another important feature to analyze is how large structures such as the Cepheus spurn present in the UMS sample clearly disappear in the RC maps. It is worth mentioning that the while the large scale structure of the Perseus and Carina-Sagittarius arms persists, the local arm has a doubtfull structure in the RC sample. This can be seen in the panels C and F from Fig. 1 While the Cepheus spur (surrounded by the big ellipsoid) and Vela (surrounded by the small ellipsoid) can be recognized in A, there is almost no trace from them in panel F, even though the ellipsoids remain in the same position.

IV. CONCLUSIONS AND FUTURE WORK

If we make a compilation of the analyzed information, we are able to conclude that, inside the thin disc:

- The over/under-density maps we have generated, and its interpretation, allow us suggest that the mechanism controlling the spiral arms in the Galactic disk, slightly displace over time the locus of the old stars respect to the young ones. For sure this statement needs to be corroborated in future analysis.

- Additionally, in this work, and using the same strategy, tools and parameters, we have quantified the differences in the over/under-densities of the two stellar populations, the UMS and the RC stars. These differences seems to trace a continuous structure with a pitch angle larger than the one derived from maser tracers.

As expected, the structures such as the Cepheus spurn and Vela Association have no overdensity counterpart in the RC sample. This introduce large uncertainties in the locus and nature of the local arm.

It is our purpose, as a next step, to define, implement and test some parameters accounting for the error in the under/over-density defined here. This indicator of dispersion is mandatory, among others, to quantify the amplitude of the spirals or to test the fiability of the derived density maps at each point. Bootstrap techniques or well defined and controlled HR subsets could be used for that purpose.

Acknowledgments We thank F. Anders for provided us data still unpublished. I am very grateful with Francesca Figueras for guide me in this project, solve any doubt and make me like astronomy and astrophysics more. And last but not least, my family that has always supported me.

V. APPENDIX

Fig.4 shows the spatial distribution of the RC stars selected as described in Sect. II C. Data from StarHorse DR2 [5], limited to $G < 18$, were obtained from CDS (total of 2.043.219 RC sources). In this case the astrometric quality flag to select "good" astrometric sources was no applied (see [7]). New data from StarHorse EDR3 [6], reaching now $G = 18.5$, has kindly been supplied by the author on June 4th, 2021. In this case an additional cut for "fidelity flag" > 0.98 ([7]) has been applied. The final sample of RC stars contain 2.463.883 sources. Improvements from DR2 to EDR3 are clearly evident in this figure, the ring-like feature between 2-3 kpc reported in [7] (see their Fig. 8) and discussed in [8], mostly provoked by a wrong use of the Gaia bad astrometric solutions in the computation of the Bayesian distances, has almost disappeared. New artificial features has been identified and reported to the authors. In particular, when analyzing subsets of 100K effective temperature interval in the rang [4500,5000]K some new over/underdensities depending mostly on galactic latitude have been detected. We hypothesize that these trends could be probably correlated with the high variable total-to-selective extinction ratio ($R(V)$) in the APOGEE data used to train the Bayesian approach in [6]. We have checked that these new effects do not affect the use of the global sample of RC stars in Sect. III.

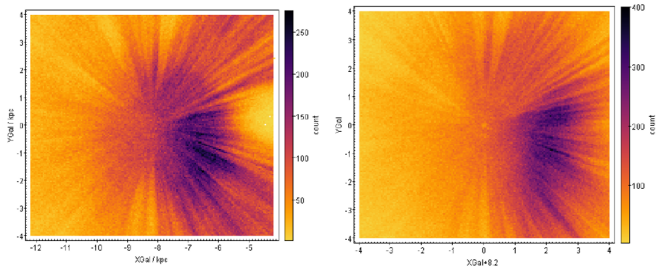

(a) StarHorse DR2 (b) StarHorse EDR3

FIG. 4: Red Clump stars distribution in the XY plane: StarHorse DR2 [5] (left) and StarHorse EDR3 (right)

[1] E. Poggio, R. Drimmel, T. Cantant-Gaudin, et al. 2021 *Galactic spiral structure revealed by Gaia EDR3*, A&A, send, arXiv:2103.01970

[2] E.D. Feigelson & G.J. Babu, 2012, in *Modern Statistical Methods for Astronomy*

[3] M.J. Reid, K.M. Menten, A. Brunthaler et al. 2019, *Trigonometric Parallaxes of High-mass Star forming Regions: Our View of the Milky Way*,ApJ **885**, 131

[4] M. Pantaleoni-González, J. Maíz-Apellániz, R.H. Barbà, et al. 2021, *The Alma catalogue of OB stars - II. A cross-match with Gaia DR2 and an updated map of the solar neighbourhood*, MNRAS, **504**, 2968

[5] F. Anders, A. Khalatyan, C. Chiappini et al., 2019, *Photo-astrometric distances, extinctions, and astrophysical parameters for Gaia DR2 stars brighter than G = 18*, A&A, **628**, A94

[6] F. Anders, et al. C. Khalatyan, A.B. Queiroz, 2021, *Photo-astrometric distances, extinctions, and astrophysical parameters for Gaia EDR3 stars brighter than G = 18.5*, A&A, in preparation

[7] J. Rybizki, G.M. Green, H. -W. Rix, et al., 2021, *A classifier for spurious astrometric solutions in Gaia EDR3*, astro-ph.IM, arXiv:2101.11641

[8] E. Zari, H. -W. Rix, N. Frankel et al., 2021, *Mapping luminous hot stars in the Galaxy*, A&A **650**, A112

[9] E. Schlafly, J.E.G. Peek, D.P. Finkbeiner et al., 2017, *Mapping the extinction curve in 3D: structure on kiloparsec scales*, ApJ §38, 36

[10] M. Monguió, P. Grosbøl, F. Figueras, 2015, *First detection of the field star overdensity in the Perseus arm*, A&A **577**, 142

[11] J.P. Vallée, 2014, *Catalog of Observed Tangents to the Spiral Arms in the Milky Way Galaxy*, ApJS, **215**, 1